PNAS Nexus, 2023, 2, 1–10
https://doi.org/10.1093/pnasnexus/pgad211
Advance access publication 23 June 2023
Research Report

Cyclic anthraquinone derivatives, unique G-quadruplex binders, selectively induce cancer cell apoptosis and inhibit tumor growth

Hikaru Fukuda [a,b,1], Tingting Zou [c,1], Satoshi Fujii [d,1], Shinobu Sato [c,1], Daiki Wakahara[c], Sen Higashi[a], Ting-Yuan Tseng[e], Ta-Chau Chang [e], Naomi Yada[f], Kou Matsuo[f], Manabu Habu[b], Kazuhiro Tominaga[b], Hiroshi Takeuchi [a,*] and Shigeori Takenaka [c,*]

[a]Division of Applied Pharmacology, Department of Health Promotion, Kyushu Dental University, Fukuoka 803-8580, Japan
[b]Division of Oral and Maxillofacial Surgery, Department of Science of Physical Functions, Kyushu Dental University, Fukuoka 803-8580, Japan
[c]Department of Applied Chemistry, Kyushu Institute of Technology, Fukuoka 804-8550, Japan
[d]Department of Bioscience and Bioinformatics, Kyushu Institute of Technology, Fukuoka 820-8502, Japan
[e]Institute of Atomic and Molecular Sciences, Academia Sinica, Taipei 10617, Taiwan
[f]Division of Oral Pathology, Department of Health Promotion, Kyushu Dental University, Fukuoka 803-8580, Japan
*To whom correspondence should be addressed: Email: shige@che.kyutech.ac.jp; r12takeuchi@fa.kyu-dent.ac.jp
[1]H.F., T.Z., S.F., and S.S. contributed equally to this work.
Edited By: Dennis Discher

Abstract

Cyclic anthraquinone derivatives (cAQs), which link two side chains of 1,5-disubstituted anthraquinone as a threading DNA intercalator, have been developed as G-quartet (G4) DNA-specific ligands. Among the cAQs, cAQ-mBen linked through the 1,3-position of benzene had the strongest affinity for G4 recognition and stabilization in vitro and was confirmed to bind to the G4 structure in vivo, selectively inhibiting cancer cell proliferation in correlation with telomerase expression levels and triggering cell apoptosis. RNA-sequencing analysis further indicated that differentially expressed genes regulated by cAQ-mBen were profiled with more potential quadruplex-forming sequences. In the treatment of the tumor-bearing mouse model, cAQ-mBen could effectively reduce tumor tissue and had less adverse effects on healthy tissue. These results suggest that cAQ-mBen can be a potential cancer therapeutic agent as a G4 binder.

Keywords: quadruplex, cyclic anthraquinone derivatives, cancer, antitumor agent, xenograft

Significance Statement

Chemotherapeutic strategies for the effective management of cancer are required. We have succeeded in developing a drug with enhanced Q-quartet selectivity by cyclic anthraquinone, a threading intercalator that has long been expected to be an anticancer agent. The mechanism of action is expected to be significant, in that it can be explained in a unified manner from in vitro to in vivo. This molecular design is expected to contribute to research in this field.

Introduction

Classical chemotherapy remains the treatment of choice for many malignancies that cannot be cured solely by surgery, which can be best used by understanding the principles of pharmacology, tumor biology, and drug resistance (1, 2). Unfortunately, chemotherapy drugs, such as some DNA alkylating agents and intercalating agents, indiscriminately kill tumor and normal cells alike and cause several adverse effects, including bone marrow suppression, gastrointestinal problems, and alopecia (3).

Hence, targeted therapies are now a component of many types of cancer therapeutics. Combining conventional chemotherapy with targeted cancer therapy may result in a more catastrophic cell kill in tumors than in healthy tissues and avoid the development of primary or secondary resistance (4, 5). Regarding targeted cancer therapy, except for the well-known mutant kinase or particular cancer microenvironment targeting (6–8), expression abnormalities of some specific genes, such as the *MYC* oncogene, which drives increased cellular proliferation, and *TERT*, which accelerates the activity of telomerase in elongating telomere DNA, are also highly correlated with carcinogenesis and could be promising targets for cancer-selective therapy (9–11).

With the increasing progress of genome sequence profiling, a higher order DNA structure, formed from Hoogsteen hydrogen bonding of guanines to form stacked quartets, also termed the G-quadruplex (G4) structure, was identified as comprehensively

Competing Interest: The authors declare no competing interest.
Received: April 4, 2023. **Revised:** May 23, 2023. **Accepted:** June 14, 2023

located and formed in the promoter regions of the above-mentioned cancer-related genes and could be involved in the regulation of gene expression and transcription (12–14). Furthermore, telomere DNA consists of repeating TTAGGG elements and can adopt multiple G4 structures, which physically inhibit the activity of telomerase and lead to antitumor effects (15, 16). Small molecules can stabilize G4 DNAs, thus causing transcription repression and triggering cancer cell apoptosis because of the functional relationship between telomeres, oncogenes, and cancer; therefore, this is a promising targeted chemotherapeutic strategy (17–24). Several molecules have been developed and identified as G4 binders, through their interaction with the G4 plane (25). However, the selectivity issues of the G4 binder interacting with particular G4 structures and exhibiting selective bioactivity for tumor cells remain incompletely explored (26).

Naphthalene diimide (NDI) derivatives are known to form stable complexes with duplex DNA by threading intercalation and have been expected to be an anticancer agent. Recently, they have been shown to bind strongly to both an electron-deficient NDI aromatic plane and electron-rich G4 plane, providing a mechanism for their anticancer activity (27–29). The performance of di-substituted NDI as anticancer agents has been improved by making them tri- or tetra-substituted, thereby inhibiting their binding to duplex DNA and increasing their specificity to G4 (29). We have successfully synthesized a cyclic NDI by linking two substituent positions of a di-substituted NDI. The cyclic form of the NDI prevents the duplex DNA from binding in a stitched fashion due to steric hindrance, thereby realizing G4-specific binding (28).

Another well-known DNA-threading intercalators, namely, anthraquinone derivatives with two substituents above and below their long axis (AQs), shows a preference for GC base pairs and disrupts DNA replication and transcription (30). Its derivatives such as doxorubicin and nogalamycin have been adopted as classical chemo-cancer therapeutic drugs but have been associated with some adverse effects such as cardiomyopathy (31, 32). AQ, like NDI, is also a G4-binding agent. It can act and is frequently reported to be effective as a telomerase inhibitor by recognizing and stabilizing the G4 structure (33–35).

This study will clarify whether G4 specificity can be expressed by cyclic AQ (Fig. 1a) and open up the possibility of anticancer agents (Fig. 1b). Here, we reported three cyclic AQ derivatives (cAQs) and investigated their G4-binding affinity and stabilization effect using UV-Vis plus Scatchard plot analysis, circular dichroism (CD) spectroscopy, and a melting temperature assay. Their performance in inhibiting telomerase activity was evaluated by using an in vitro telomerase repeated amplification protocol (TRAP) assay.

Results

cAQ-mBen might be a promising G4-selective binder

Three cAQs were prepared with different cyclic substituents, and the noncyclic anthraquinone AQ-ac was adopted as a control molecule, with an acetylated amino terminus to avoid free amino group induced–biased comparison. The synthesis and verifying information is provided in the experimental section (Figs. 1a and S1–S5). UV-Vis titrations were performed to investigate the interaction of these AQ derivatives with G4 and double-stranded oligonucleotide (ds-oligo; Figs. 2a, S6–S8, and Table S1). All derivatives showed hypochromic effects and red shifts with G4 and ds-oligo. All derivatives could be analyzed by Scatchard analysis in the interaction with G4 using absorbance changes; however, the ds-oligo was analyzed in a Benesi–Hildebrand plot because the absorbance of the complex was not clear, except for the acyclic AQ-ac. Although the exact binding capacity for ds-oligo could not be determined, it was suggested that the cAQ derivative exhibits hundreds of times higher G4 specificity than ds-oligo. Adding these AQ derivatives to telomere G4 with potassium ion, cAQs induced a shift in CD spectra with increased intensity around 245 and 288 nm and decreased intensity around 257 nm (Figs. 2b and S9). A similar phenomenon has been reported in a previous anthraquinone study (36); cAQ-mBen induced the most significant CD shift, indicating a stronger G4 structure strain might be generated because of cAQ binding.

Then, CD-based melting temperature measurements investigated the stabilization effects of AQ derivatives for G4 and ds-oligo. Interestingly, for telomere G4 within 100 mM K^+, AQ-Ac did not stabilize its structure, cAQ-C2 and cAQ-ch enhanced the melting temperature by 2.8°C, and cAQ-mBen led to the strongest stabilization and enhanced the melting temperature by 8.8°C. For telomere G4 within 100 mM Na^+, cAQ-mBen was still able to induce a stronger stabilization for G4 than other AQ derivatives (Figs. 2c, d, S10, and Table S2). According to the molecular model created using Molecular Operating Environment (37), when cAQ-mBen recognizes telomere G4 (PDB, 2GKU), the cyclic structure of cAQ-mBen serves as a pocket for adenine insertion, and the meta-benzene part can also form a hydrogen bond with the nucleic base, enhancing the binding affinity of cAQ-mBen for G4 (Fig. 2e). Considering that cAQ-mBen also demonstrated the highest binding constant, cAQ-mBen is a promising G4-selective binder with enhanced affinity for recognizing and stabilizing G4 structures.

cAQ-mBen inhibited telomerase activity in vitro and recognized G4 in vivo

AQ derivatives stabilize the G4 structure and further inhibit the function of telomerase. Here, a classical gel shift assay was combined with TRAP assay to investigate the telomerase inhibition ability of these AQ derivatives (32, 35, 36). Upon increasing the concentration of AQs, telomere DNA elongation was inhibited, as seen by the decreases in shifting bands (Fig. 3a). Consistent with the results obtained for the melting temperature measurement, cAQ-mBen displayed the strongest inhibition ability, which induced a significant inhibition of telomere DNA elongation, whereas cAQ-C2 and cAQ-ch and AQ-Ac inhibited telomerase activity marginally. This finding indicated that the ability of G4 binder to stabilize telomerase G4 could be a positive factor for further inhibiting telomerase activity. Therefore, cAQ-mBen was considered to have a higher potential to interfere with the function of telomerase and induce a shorter length of telomere DNA. Nevertheless, AQ-Ac did not significantly influence the telomere DNA elongation within 10 μM, but the continuous increasing concentration of AQ-Ac might cause DNA aggregation and disturb the DNA gel shift (Fig. S11). Furthermore, cAQ-mBen, cAQ-C2, and cAQ-ch did not inhibit PCR up to 50, 150, and 150 μM, respectively (Fig. S11), indicating weak interaction with duplex DNA. This result is in agreement with the binding results based on UV-Vis measurements (Fig. 2a, Table S1).

To examine whether cAQ-mBen can recognize G4 DNA in the cells, we performed a G4 binder competition assay with fluorescence lifetime imaging microscopy according to a previous report (38). The G4 DNA was revealed by o-BMVC, a G4 fluorescent probe, to selectively recognize the G4 structure. The pretreatment of

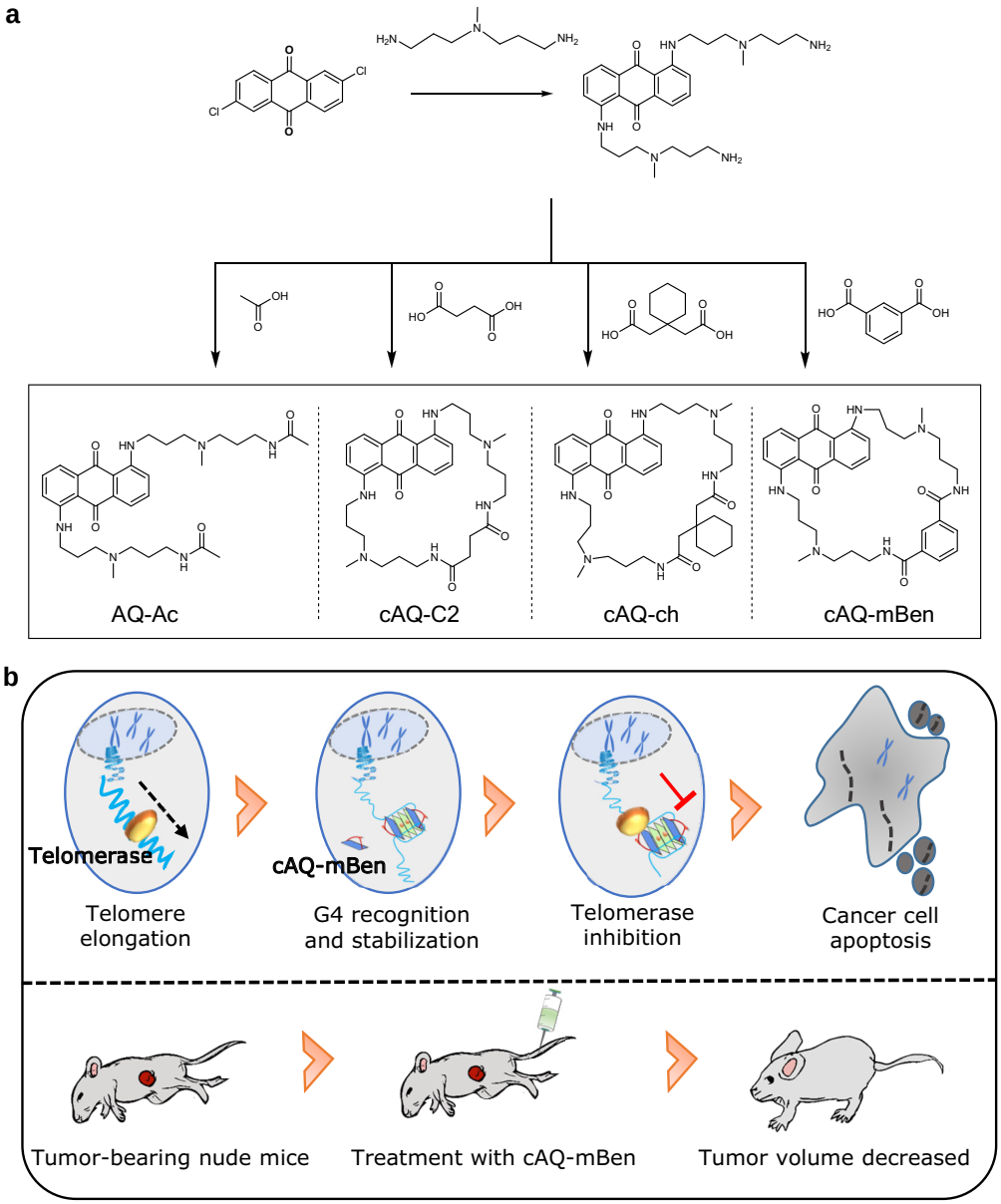

Fig. 1. G-quadruplex binder for targeted cancer therapeutic application. a) Anthraquinone derivatives synthesis scheme. b) Supposed activity of anthraquinone derivatives for cancer therapeutic application.

HeLa cells with cAQ-mBen resulted in a 65% reduction in the number of *o*-BMVC foci in the nucleus (Fig. 3b and c), indicating that cAQ-mBen could block the subsequent binding of *o*-BMVC to G4s, similar to previous findings for other G4-binding molecules (39). The results have established that cAQ-mBen could bind to G4 DNA in the cells.

cAQ-mBen selectively inhibited cancer cell proliferation

The cell proliferation assay was performed with several cell lines, and the half maximal inhibitory concentration (IC_{50}) values were calculated to clarify whether these AQ derivatives have the potential to selectively inhibit only tumor cell proliferation (Table 1, Fig. S12). cAQ-mBen showed a potent ability to inhibit cancer cell proliferation with IC_{50} values generally <1 μM and less toxicity to normal cells such as freshly prepared primary mouse bone marrow cells (BMCs) and cell lines derived from healthy tissue (IC_{50} > 6 μM), especially the IC_{50} for HeLa was only 0.3 μM, which was almost 20-fold lower than for normal cells. The other two cAQ derivatives, cAQ-C2 and cAQ-ch, showed comparable G4-binding affinity but weaker telomere G4 stabilization effect and telomerase inhibition ability, with unsatisfactory results in terms of inhibiting cancer cell proliferation and differentiating cancer and normal cells. Moreover, AQ-Ac could selectively inhibit the proliferation of cancer cell lines and not normal cells. Here we also compared the inhibitory effect of AQs with cisplatin (cis-diamminedichloroplatinum(II), CDDP), one of the most commonly used cancer chemotherapeutic drugs (40). However, the DNA-damaging agent CDDP showed comparable or even stronger inhibitory effect on the proliferation of healthy cells than that of cancer cell lines such as Ca9-22 and SAS cells (Table 1, Fig. S12), which further demonstrated that cAQ-mBen has a superior effect on cancer-selective growth inhibition as a G4-targeted agent.

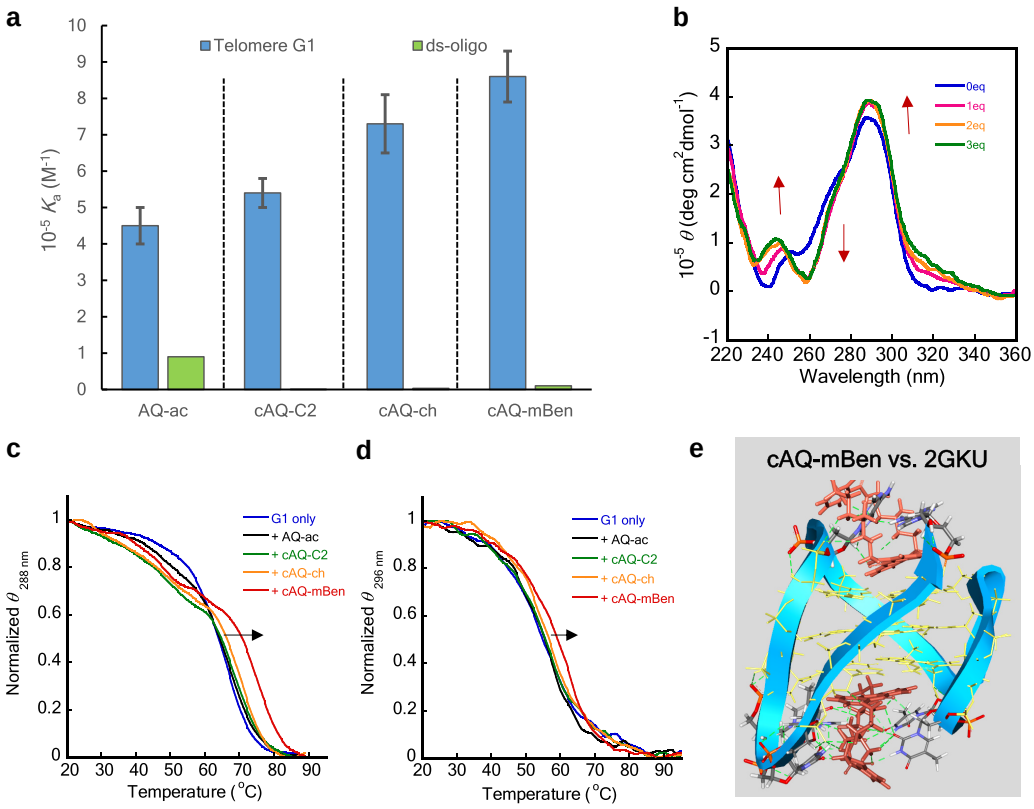

Fig. 2. Anthraquinone derivatives recognize and stabilize G-quadruplex. a) Binding affinity of AQ derivatives for telomere G1 and ds-oligo; buffer: 100 mM KCl and 50 mM Tris-HCl (pH 7.4). b) CD spectra of 1.5 μM telomere G1 with 0-4.5 μM cAQ-mBen; buffer: 100 mM KCl and 50 mM Tris-HCl (pH 7.4). c) Melting temperature profile of 1.5 μM telomere G1 with 4.5 μM of anthraquinone derivatives; buffer: 100 mM KCl and 50 mM Tris-HCl (pH 7.4). d) Melting temperature profile of 1.5 μM telomere G1 with 4.5 μM of anthraquinone derivatives; buffer: 100 mM NaCl and 50 mM Tris-HCl (pH 7.4). e) Binding modeling of cAQ-mBen with telomere G-quadruplex (PDB, 2GKU).

cAQ-mBen regulated the gene expression profile

Then, to address the gene regulation difference between cAQ-mBen and AQ-Ac, RNA-sequencing (RNA-Seq) analysis was conducted by treating the tumor cell line SAS with 1 μM of AQ-Ac or cAQ-mBen for 6 or 24 h and then plotting the differential expression of genes to investigate the gene expression profile. Unexpectedly, no gene expression fluctuation was observed after AQ-Ac treatment; however, cAQ-mBen treatment markedly induced differential gene expression (Data set Fig. 4; PNASNEXUS-PNASNEXUS-2023-00340R-s05.xlsx. More differentially expressed genes (DEGs) were identified after 5 μM cAQ-mBen treatment than after 1 μM cAQ-mBen treatment and at 24 h than at 6 h. For all cAQ-mBen treatment conditions, 262 DEGs (3.5%) were obtained (Fig. 4a).

To further investigate possible correlations between cAQ-mBen-induced gene expression modulation and the G4 region, the potential quadruplex-forming sequences (PQSs) of the genome were predicted using G4Hunter (41). The distribution of the numbers of PQS on the promoter region (from −1 to 1 kb) and gene body was compared between upregulated and downregulated genes after cAQ-mBen treatment under various conditions (Fig. 4b). The numbers of PQS in DEGs were higher than those in all genes in the background. For the promoter, the distribution of PQS in the gene with downregulated expression was slightly larger than that in the gene with upregulated expression at 6 h; however, at 24 h, the difference had almost disappeared. For the gene body, when 5 μM of cAQ-mBen was added, the distribution of PQS in the genes with downregulated expression was larger than that in the genes with upregulated expression at both 6 and 24 h, whereas there were minor differences after 1 μM cAQ-mBen treatment.

According to the results of the Kyoto Encyclopedia of Genes and Genomes (KEGG) pathway enrichment analysis (Fig. 4c), for genes with upregulated expression, cancer-related pathways, virus infection–related pathways, p53-signaling pathways, apoptosis, and cellular senescence involved in tumor suppressor pathways were highly enriched. In contrast, genes with downregulated expression were enriched in many pathways involved in diseases of the nervous system such as Alzheimer's, Parkinson's, and prion disease. These pathways were associated with oxidative phosphorylation (OXPHOS), which occurs inside the mitochondrion. Figure 4d shows the expression levels and the number of PQS on the genes that are related to telomere extension by telomerase, which is identified as R-HSA-171319 in the Reactome database (42), such as *TERT* and *POT1*; these results indicate that cAQ-mBen affects the biogenesis and assembly of the telomerase RNP and their recruitment to the telomeric chromosome end.

cAQ-mBen inhibited cell proliferation in correlation with *TERT* expression and induced cancer cell apoptosis

Subsequently, to address whether the inhibitory effect of cAQ-mBen is correlated with telomerase activity inhibition, we

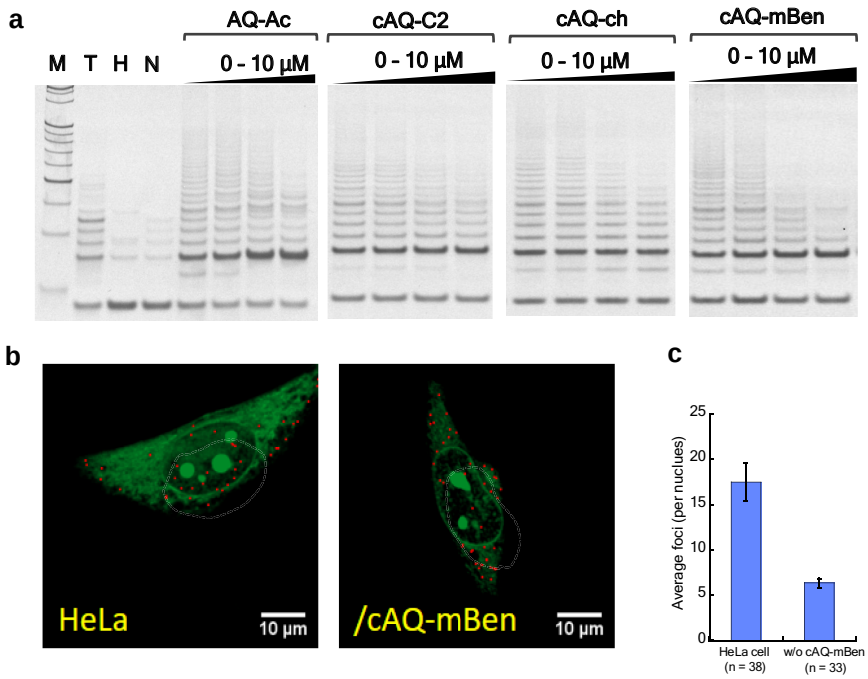

Fig. 3. cAQ-mBen inhibits telomerase activity in vitro and recognizes G-quadruplex in vivo. a) Telomerase activity inhibition by AQ derivatives in a TRAP assay. Increasing concentrations of AQs were added to the TRAP mixture in the presence of an internal control and analyzed using gel electrophoresis (M: 20 bp step Ladder, T: TSR8 used as a template, H: lysate from heat-treated HeLa cells, N: no HeLa cells). b) Binary images of the o-BMVC foci in HeLa cells (left) and HeLa cells incubated with 5 μM cAQ-mBen overnight (right). c) Quantitative analyses of the number of o-BMVC foci in the pretreated HeLa cells without or with 5 μM cAQ-mBen.

investigated the *TERT* mRNA expression levels in different cancer cell lines, immortalized cell lines, and normal cells, which is a rate-limiting determinant for controlling telomerase activity (43). In the normal human epidermal keratinocytes (NHEKs) and BMCs, both of which were primarily prepared cells from healthy tissues, the human *TERT* or mouse *Tert* mRNA expression was hardly detected compared with that in the human cancer cell line Ca9-22 or immortalized mouse cell lines MC3T3-E1, respectively (Fig. 5a), and a clear stronger cell proliferation inhibition was observed for Ca9-22 than for the other two primary cells from healthy tissues (Fig. 5b). Then, we investigated the relationship between the expression level of *TERT* and the effect of cAQ-mBen in four different human cancer cell lines. The mRNA expression levels of *TERT* in Ca9-22 and HeLa cells were significantly higher than those in HEK293 and HSC-2 cells (Fig. 5c). Proliferation of all cancer cells was inhibited in a dose-dependent manner that was positively correlated with the *TERT* expression level in these cell lines, indicating that cAQ-mBen potently inhibited the proliferation of telomerase-active cell lines (Fig. 5d).

Since cAQ-mBen inhibited cell growth with higher specificity in cancer cells than normal cells and gene expression profile in the RNA-Seq analysis indicated the state of apoptosis after cAQ-mBen treatment in these cell lines, we sought to determine whether the potent cell proliferation inhibitory effect was mediated through induction of cell death or not. Tumor cell line SAS was incubated with cAQ-mBen or CDDP (as a positive control) and then subjected to an annexin V/propidium iodide (PI)-staining assay. When the cells were incubated with 5 μM of cAQ-mBen for 24 h, around 10.5% of the cells were positive for annexin V (representing the cells in the early apoptotic stages) and 10.9% of the total cells were positive for PI signal (which stains necrotic cells), both were at a comparable level with that of SAS incubated with 50 μM CDDP (24.0 and 18.5%, respectively; Fig. 5e).

RNA-Seq analysis suggested that cAQ-mBen regulated many caspase-related genes; regarding the protein level, after 5 μM cAQ-mBen or 50 μM CDDP treatment, the digestion of poly (ADP-ribose) polymerase-1 (PARP-1) and caspase-3 was observed in a time-dependent manner, i.e. intact forms of both PARP-1 and caspase-3 were decreased along with increasing amount of cleaved PARP-1 (Fig. 5f). These results further suggested that cAQ-mBen could induce cancer cell apoptosis.

cAQ-mBen suppressed tumor growth without obvious adverse effect in a mouse xenograft model

We next investigated the effect of cAQ-mBen on tumor growth and its adverse effects in vivo, with continuous adaptation of CDDP as a chemotherapeutic control. Stable SAS cell mouse xenograft models were prepared in our laboratory for evaluation. Based on the potent antitumor effects observed with cAQ-mBen in the cell viability assays, 3 μmol/kg of cAQ-mBen and 30 μmol/kg of CDDP were utilized for treating tumor-bearing mice. The tumor volume continuously increased without treatment; however, the increase in the tumor volume was significantly suppressed in mice treated with cAQ-mBen and CDDP (Fig. 6a, b and S13). The effect of cAQ-mBen on suppressing tumor growth was comparable with that of CDDP despite the use of a 10-fold lower dose than CDDP. Although CDDP considerably reduced the body weight of mice, cAQ-mBen barely affected the body weight throughout the study period (Figs. 6c and S13).

CDDP is known to induce a pathological change in the liver and kidney of mice: the shape of the central vein of the liver becomes irregular, the size of the glomerulus becomes smaller, and the cell

Table 1. Cytotoxicity of AQ derivatives for different cell lines.

Chemotherapy agents	$IC_{50}/\mu M$						
	Cancer cell line					Normal cells	
	HeLa	Ca9-22	SAS	HSC-2	HEK293	ASF-4-4L2	BMC
AQ-ac	1.4	1.1	0.5	0.5	0.9	5.4	6.0
cAQ-C2	>20	>20	>20	>20	>20	8.2	>20
cAQ-ch	5.5	>20	>20	>20	6.3	>20	>20
cAQ-mBen	0.3	0.4	0.6	1.0	1.4	6.3	6.3
CDDP	0.5	27.7	4.3	—	—	—	1.3

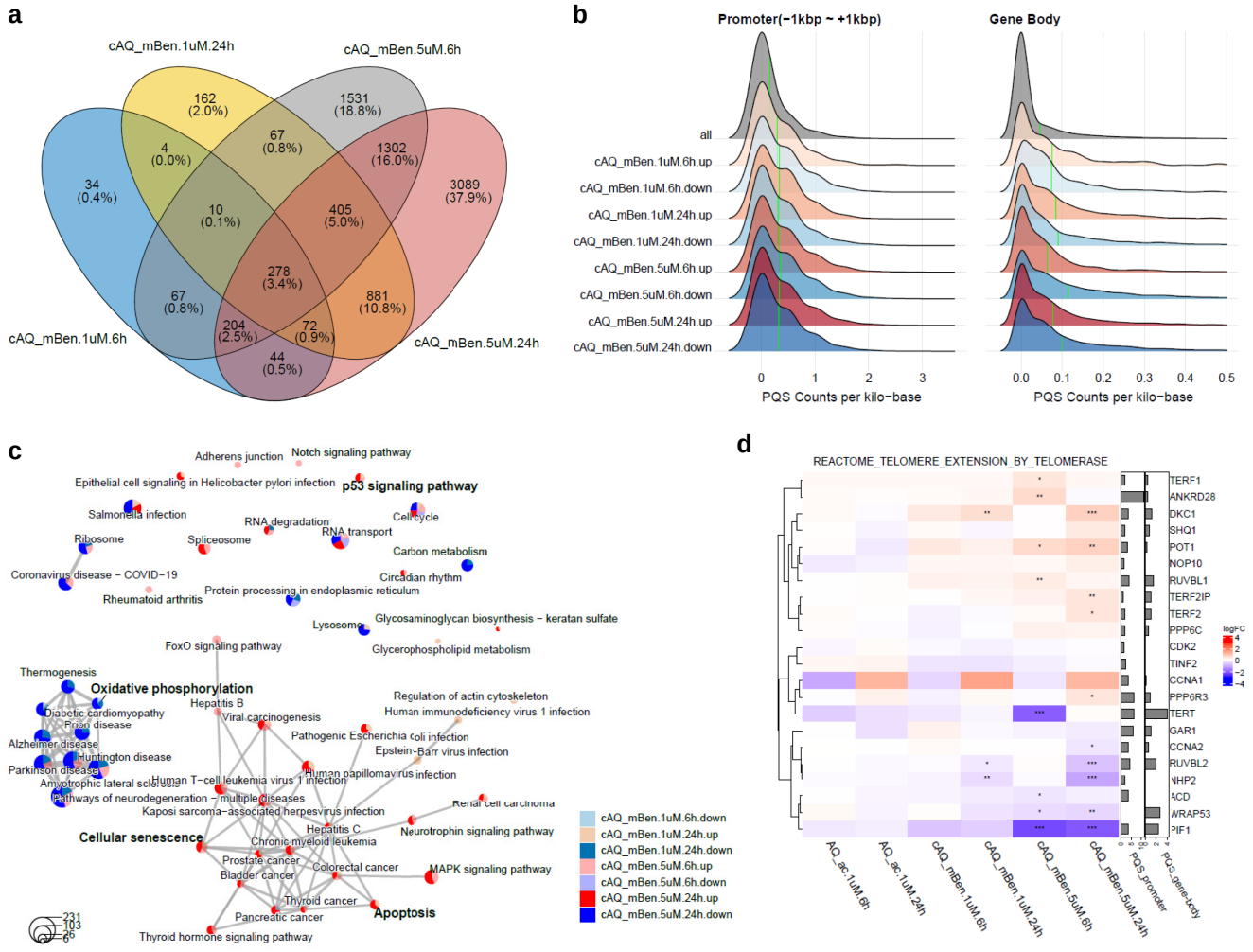

Fig. 4. cAQ-mBen regulates gene expression as seen by using RNA-Seq analysis. a) Venn diagram of DEGs induced by cAQ-mBen treatment. b) The distribution of the number of PQS in the promoter region (−1 to 1 kb) and gene body of genes with upregulated and downregulated expression after cAQ-mBen treatment. The vertical lines are mean values. c) KEGG pathways associated with cAQ-mBen treatment. Each node represents an enriched KEGG pathway. The size of the node indicates the number of genes enriched in the pathway. Two nodes connected by an edge have similar enriched genes. d) The heatmap of the logFC values of the genes related to telomere extension by telomerase from the Reactome database, and the bar plot indicates the PQS counts per kilobase on promoter and gene body. The asterisks represent the false discovery rate (FDR) used for the differential gene expression analysis using edgeR (*FDR < 0.05, **FDR < 0.01, ***FDR < 0.001).

arrangement of the glomerulus becomes irregular (44). In our evaluation, similar pathological changes in the liver and kidney including significant condensation of the glomerulus area were observed in mice treated with CDDP (Fig. 6d and e). In contrast, no histopathological changes were observed in the liver of mice treated with cAQ-mBen. The cell arrangement and the size of the glomerulus in the kidney of cAQ-mBen-treated mice were also not affected (Fig. 6d and e). Moreover, CDDP treatment led to a substantial increase in various physiological indices (BUN, UA, AST, ALT, CRE, and γ-GTP levels), as seen by performing biochemical examination of the blood serum samples, indicating damage to the liver and kidney. However, no significant differences in terms of these indices were observed between cAQ-mBen treatment and negative control groups, indicating that cAQ-mBen did not affect these organs (Fig. 6f, Table S3). These results suggest that cAQ-mBen shows a strong suppressing effect on

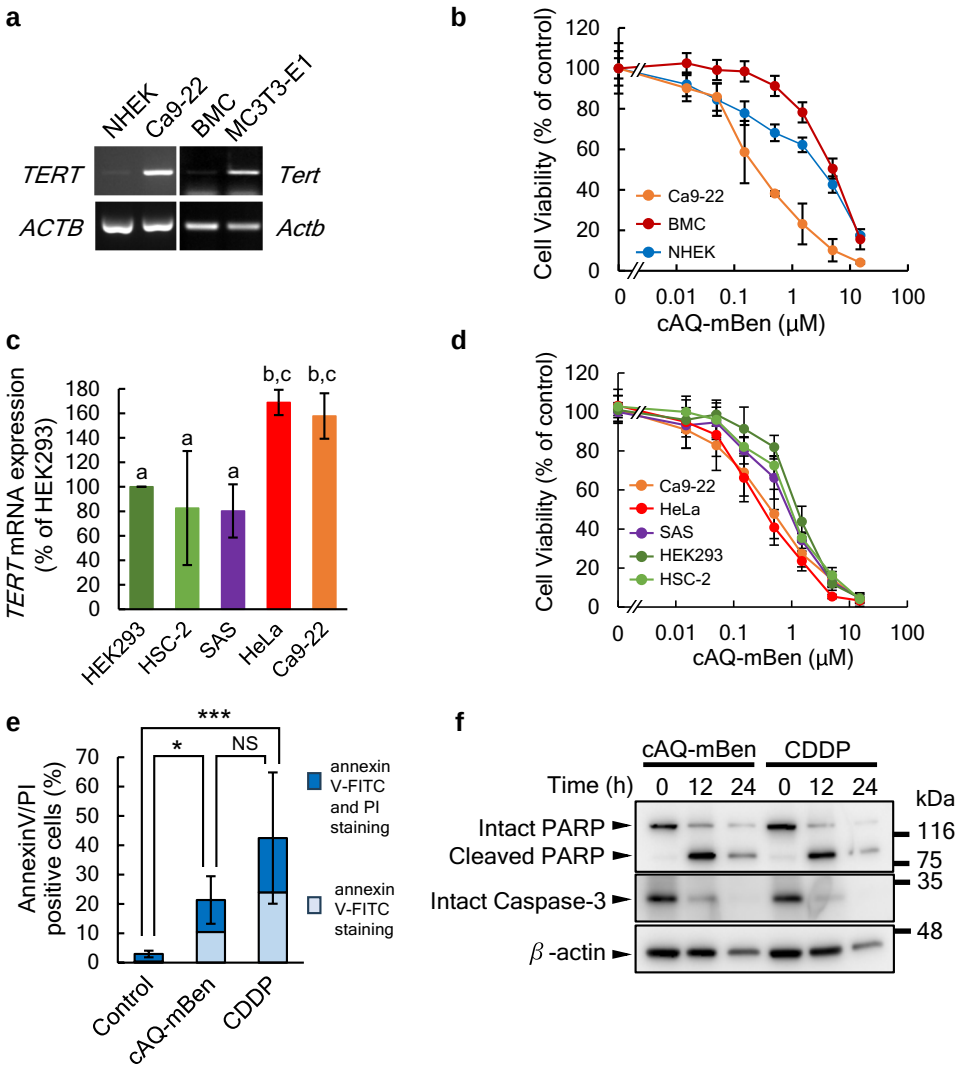

Fig. 5. cAQ-mBen inhibits cell proliferation and induces cell apoptosis. a) Expression of human TERT or mouse Tert mRNA in the primarily prepared normal cells—NHEKs and mouse BMCs—was compared with those of tumor-derived or immortalized cell lines—human gingival carcinoma cell line (Ca9-22) and mouse osteoblast-like cell line (MC3T3-E1) by general PCR. b) Cell viabilities of NEHK, BMCs, and Ca9-22 cells treated with the indicated concentrations of cAQ-mBen for 48 h. Data are presented as mean values ± SD. c) TERT mRNA expression of human tumor or immortalized cell lines, HEK293, HSC-2, SAS, HeLa, and Ca9-22 were assessed by qPCR analysis. Data are presented as mean values ± SD ($n = 4$). Same letters indicate no significant difference in the group (a, b, c), while different letters indicate significant difference: b, $P < 0.05$ versus HEK293; c, $P < 0.01$ versus HSC-2 or SAS. Statistical significance was calculated using one-way ANOVA followed by Tukey's multiple comparisons test. Exact P-values are available in source data. d) Cell viabilities of Ca9-22, HeLa, SAS, HEK293, and HSC-2 cells treated with the indicated concentrations of cAQ-mBen for 48 h. Data are presented as mean values ± SD. e) Increase in annexin V/PI staining of the cells after 5 μM cAQ-mBen or 50 μM CDDP treatment for 24 h. Cells positive to annexin V-FITC staining alone and cells double positive to both annexin V-FITC and PI staining were expressed as % of total cell numbers in each objective field. Data are mean values ± SD of total apoptotic cells ($n = 5$). One-way ANOVA followed by Tukey's multiple comparisons test was used to assess significance. *$P < 0.05$, ***$P < 0.001$; NS, not significant (control versus cAQ-mBen, $P = 0.0112$; control versus CDDP, $P = 0.0002$, cAQ-mBen versus CDDP, $P = 0.0803$). f) Western blot analysis of caspase-3 and PARP-1 cleavages, as induced by cAQ-mBen or CDDP. SAS cells were treated with 5 μM cAQ-mBen or 50 μM CDDP for 12 or 24 h and subjected to western blot analysis.

tumor growth in vivo, which is comparable with that of CDDP, but is more tumor specific with less adverse effects.

Discussion

We developed three cAQs (cAQ-C2, cAQ-ch, and cAQ-mBen) and succeeded in improving the specificity of cAQs for recognizing G4 compared with noncyclic AQ. In particular, cAQ-mBen showed the highest stabilizing effect on telomeric G4 and the strongest inhibition of telomerase activity. *o*-BMVC competition experiments showed that cAQ-mBen is taken up into cells simply by adding it to cells and binds to the nuclear G4 site. Furthermore, it showed excellent potential to selectively inhibit tumor cell growth.

G4 targeting has been considered one potential strategy for targeted cancer therapy; many G4 ligands and some ligand multimers have been developed for G4 recognition in vitro and in vivo. Some previously reported small molecule inhibitors of rDNA transcription mediate their function by interacting with the G4 structure (19). However, most of these molecules continue to be investigated in vitro, and only a few reports of satisfactory antitumor effects were obtained in clinical trials (45, 46). Binding affinity and structure stabilization are two important in vitro factors to assess the performance of the G4 ligand for G4 targeting. However, some G4 ligands demonstrated promising potential for G4

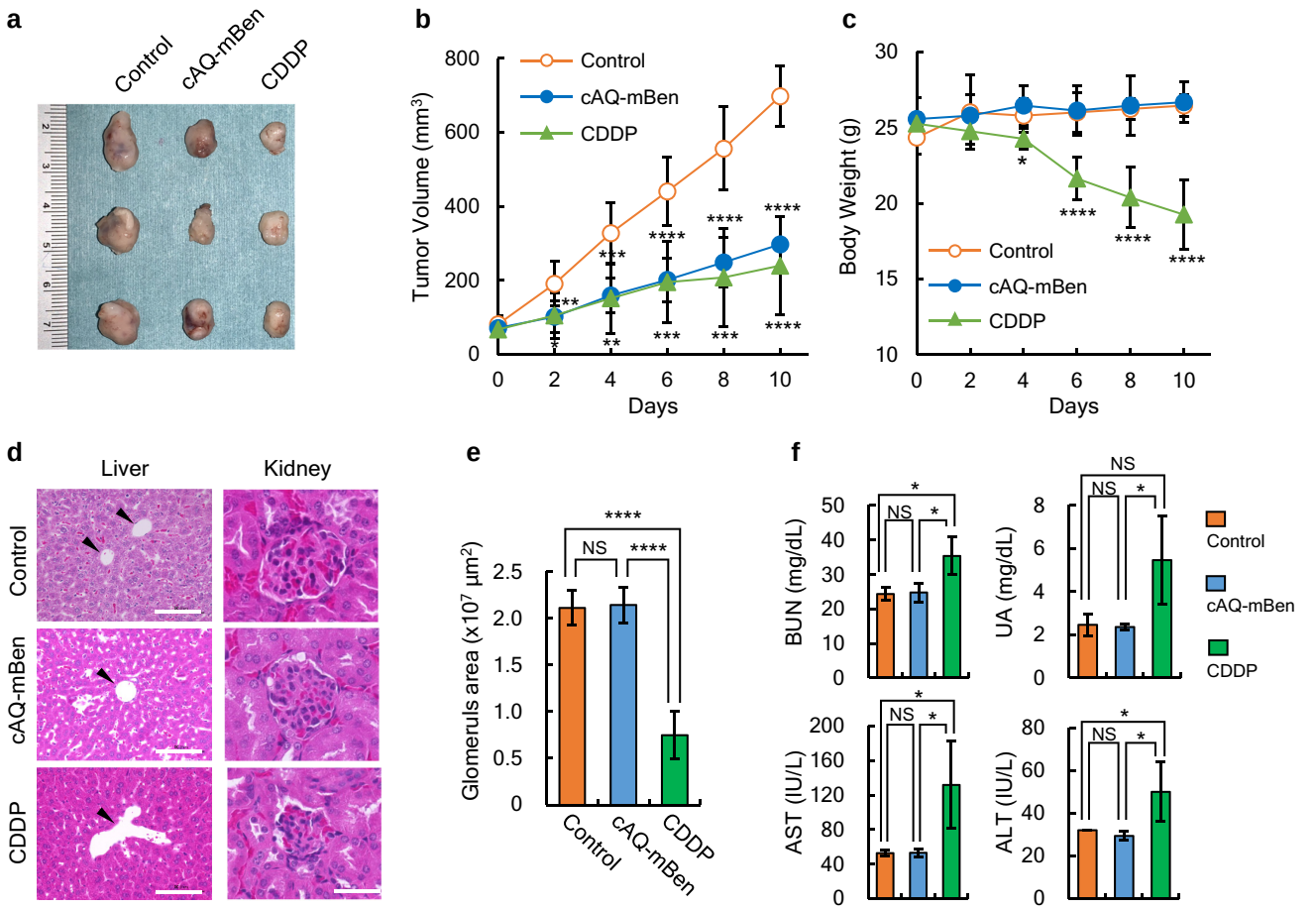

Fig. 6. cAQ-mBen suppressed tumor growth with no obvious adverse effect in a mouse xenograft model. Mouse xenograft model was established by subcutaneously inoculating SAS cells into KSN/Slc nude mice. Seven days after the inoculation (day 0), saline as a control, 3 μmol/kg of cAQ-mBen or 30 μmol/kg of CDDP, was peritoneally administered every 2 days for 5 times. a) Representative images are the excised tumor tissues at day 10 of cAQ-mBen or CDDP treatment. b) Tumor volume and c) body weight were measured at the indicated point and expressed as mean values ± SD ($n = 9$ for control and cAQ-mBen, and $n = 8$ for CDDP). Open circle, control; closed circle, cAQ-mBen; closed triangle, CDDP. Two-way ANOVA followed by Tukey's multiple comparisons test. $^{*}P < 0.05$, $^{**}P < 0.01$, $^{***}P < 0.001$, and $^{****}P < 0.0001$ against control mice on each day. Exact P-values are available in the source data. d to f) Effect of cAQ-mBen on pathophysiological findings in the liver and kidney tissues. Tumor-free KSN/Slc nude mice were treated with saline, cAQ-mBen, or CDDP for 10 days, the same as xenograft model mice, and then were subjected to histopathological analyses and biochemical examination of the serum. d) Atypical images of HE-stained tissue sections of hepatic lobule of the liver and glomerulus of the kidney. Arrow heads indicate central veins. Scale bar: 100 μm. e) Glomerulus area was measured and indicated as mean values ± SD ($n = 15$ sections from 3 mice). Statistical significance was calculated using one-way ANOVA followed by Tukey's multiple comparisons test. $^{****}P < 0.0001$; NS, not significant (control versus cAQ-mBen, $P = 0.9119$; exact P-values <0.0001 are not available). f) The blood was collected from mice at day 10 of cAQ-mBen or CDDP treatment, and the serum was subjected to a biochemical examination. Data are presented as mean values ± SD ($n = 3$). Statistical significance was measured using one-way ANOVA followed by Tukey's multiple comparisons test. $^{*}P < 0.05$; NS, not significant (control versus cAQ-mBen for BUN, $P = 0.9887$; UA, $P = 0.9844$; AST, $P = 0.9999$; ALT, $P = 0.9157$, and control versus CDDP for BUN, $P = 0.0244$; UA, $P = 0.0533$; AST, $P = 0.0379$; ALT, $P = 0.0774$). BUN, blood urea nitrogen; UA, uric acid; AST, aspartate aminotransferase; ALT, alanine aminotransferase.

recognition in vitro but poor performance when tested in vivo. The in vitro and in vivo evaluation gap is a conceivable but straightforward issue for chemo-targeted cancer therapeutic research.

Previously, other studies on AQ derivatives, with selectivity similar to that of cAQ-C2 and cAQ-ch but lower G4 stabilization effects, also showed the same unsatisfactory inhibition of cancer cell growth (38). However, cAQ-mBen could potently stabilize G4 structures over other cAQs and demonstrated excellent specificity for antitumor growth, indicating that this stabilization effect might be essential to its therapeutic effects. However, it is impossible to conclude that its stabilization effect is the key factor in its being a potential G4 binder. Finding the right trade-off between affinity and selectivity of G4 ligand remains an object of study in the design of G4 ligands (22). Moreover, AQ-ac also demonstrated comparable performance in selectively inducing cancer cell death, but the anticancer cell proliferation effect was not correlated with telomerase-activity-related *TERT* mRNA expression levels. Regarding the poor ability of AQ-Ac to selectively differentiate and stabilize G4 and the observed AQ-Ac-induced DNA aggregation, AQ-ac was considered to have an anticancer effect as a GC base pair-preferring DNA intercalator rather than as a G4 binder.

After cAQ-mBen treatment, the numbers of PQS in the DEGs were significantly increased in both the promoter region and gene body, suggesting that cAQ-mBen might regulate gene expression by binding to G4. PQSs were present in genes with both downregulated and upregulated expressions. The formation of G4 in the promoter does not necessarily inhibit polymerase progression and suppress gene expression. G4 chromatin immunoprecipitation-sequencing (ChIP-Seq) and assay for transposase-accessible chromatin with high-throughput sequencing results obtained by Hänsel-Hertsch et al. have also indicated that G4 sites show hallmarks of dynamic epigenetic features in

chromatin primarily found in regulatory, nucleosome-depleted regions and correlate with genes showing elevated transcription (19). Therefore, in vivo, G4 may act as a promoter or repressor depending on chromatin status and other transcription factors.

Except for the activation of apoptosis, it was characteristic that the mitochondrial OXPHOS-related genes were downregulated at 6 and 24 h with 1 and 5 μM cAQ-mBen treatment. Mitochondria are complex organelles that influence the development, growth, survival, and metastasis of cancer cells, and many aspects of mitochondrial biology other than energy production actively contribute to tumorigenesis. Recently, the metabolic, mitochondrial, and oxidative stress vulnerabilities of cancer cells have become a focus of attention as selective targets for inducing cancer cell death (47, 48). Moreover, the regulatory roles of G4 structures in mitochondria have been drawing increasing research attention (49). Like some G4-specific binding ligands that could bind to G4 in mitochondria (50, 51), it is conceivable that cAQ-mBen reported here also bound to G4 in mitochondria and suppressed OXPHOS-related gene activity, resulting in apoptosis.

A previous study (29, 52) reported changes in gene expression by RNA-Seq in human pancreatic cancer cell lines, PANC-1 and MIA PaCa-2, with the addition of NDI derivatives, CM03 and SOP1812, which are G4-binding reagents. The study showed that the G4-binding reagent downregulated many genes in the Wnt/β-catenin signaling pathway. However, in our study, the downregulated genes were not significantly overrepresented in the Wnt/β-catenin signaling pathway (cAQ-mBen, 5 μM, 6 h, 9 genes, $P = 0.96$; cAQ-mBen, 5 M, 24 h, 19 genes, $P = 0.97$). Individual gene expression changes were also different between cAQ-mBen and NDI derivatives. For example, the expression of hTERT, in which G4 is present in the promoter, was significantly downregulated once after 6 h of cAQ-mBen addition and reverted to the original level after 24 h (Fig. 4d); whereas the expression of CM03 and SOP1812 remained downregulated after 6 and 24 h, respectively. At this time, we do not know whether this is due to the difference in the cell line between human pancreatic and human tongue cancer, the difference in the G4 sequence to which the compounds bind, or some other factor.

Regarding the antitumor activity in the mouse xenograft model, cAQ-mBen showed comparable tumor-suppressing performance to that of CDDP but significantly fewer adverse effects that were assessed. In contrast, CDDP displayed serious adverse effects on the liver, kidneys, and testis, and reduced body weight. Although the antitumor activity of cAQ-mBen on cultured cells showed a tendency to correlate with the *TERT* gene expression level in the cells. G4-binding ligands do not target a specific gene or protein but various locations in the genome and interact with surrounding transcription factors to promote or inhibit gene expression via multiple pathways to display antitumor effects. Owing to the still ambiguous function of G4 in vivo, it is difficult to unravel the detailed mechanism of cAQ-mBen leading to apoptosis. Investigating the genome-wide localization of G4 using G4 ChIP-Seq4 and the binding state of cAQ-mBen to the genome by applying cAQ-mBen to Chem-Seq may give more information for elucidating the underlying regulatory process (53).

Supplementary material

Supplementary material is available at *PNAS Nexus* online.

Funding

This study was supported in part by the Nakatani Foundation for the Advancement of Measuring Technologies in Biomedical Engineering, Japan (to S.T.), and by Grants-in-Aid from the Japan Society for the Promotion of Science (JSPS) KAKENHI, Japan (JP19K15700 to T.Z., JP18K09775 to K.T., JP22K17164 to H.F., and JP19H02748 to S.T.).

Author contributions

S.S. and S.T. designed research; H.F., T.Z., S.F., S.S., D.W., S.H., T.Y.T., and N.Y. performed research; H.F., T.Z., S.F., S.S., T.Y.T., T.C.C., K.M., M.H., K.T., H.T., and S.T. analyzed data; and H.F., Z.T., S.F., S.S., H.T., and S.T. wrote the paper.

Data availability

All study data are included in the article, Data set Fig. 2, Data set Fig. 3gel, Data set Fig. 3, Data set Fig. 4, Data set Fig. 5gel, Data set Fig. 5, Data set Fig. 6, and/or SI Appendix.

References

1 Malhotra V, Perry MC. 2003. Classical chemotherapy: mechanisms, toxicities and the therapeutic window. *Cancer Biol Ther*. 2(Suppl 1):1–3.
2 Sawyers C. 2004. Targeted cancer therapy. *Nature*. 432:294–297.
3 MacDonald VC. 2009. Chemotherapy: managing side effects and safe handling. *Can Vet J*. 50:665–668.
4 Gampenrieder SP, Rinnerthaler G, Greil R. 2013. Neoadjuvant chemotherapy and targeted therapy in breast cancer: past, present, and future. *J Oncol*. 2013:732047.
5 Gerber DE. 2008. Targeted therapies: a new generation of cancer treatments. *Am Fam Physician*. 77:311–319.
6 Zhou W, *et al*. 2009. Novel mutant-selective EGFR kinase inhibitors against EGFR T790M. *Nature*. 462:1070–1074.
7 Karaman MW, *et al*. 2008. A quantitative analysis of kinase inhibitor selectivity. *Nat Biotechnol*. 26:127–132.
8 Feig C, *et al*. 2012. The pancreas cancer microenvironment. *Clin Cancer Res*. 18:4266–4276.
9 Miller DM, Thomas SD, Islam A, Muench D, Sedoris K. 2012. c-Myc and cancer metabolism. *Clin Cancer Res*. 18:5546–5553.
10 Wang L, *et al*. 2002. hTERT expression is a prognostic factor of survival in patients with stage I non-small cell lung cancer. *Clin Cancer Res*. 8:2883–2889.
11 Brooks TA, Hurley LH. 2009. The role of supercoiling in transcriptional control of MYC and its importance in molecular therapeutics. *Nat Rev Cancer*. 9:849–861.
12 Lipps HJ, Rhodes D. 2009. G-quadruplex structures: in vivo evidence and function. *Trends Cell Biol*. 19:414–422.
13 Biffi G, Tannahill D, McCafferty J, Balasubramanian S. 2013. Quantitative visualization of DNA G-quadruplex structures in human cells. *Nat Chem*. 5:182–186.
14 Bochman ML, Paeschke K, Zakian VA. 2012. DNA secondary structures: stability and function of G-quadruplex structures. *Nat Rev Genet*. 13:770–780.
15 Hansel R, Lohr F, Trantirek L, Dotsch V. 2013. High-resolution insight into G-overhang architecture. *J Am Chem Soc*. 135: 2816–2824.
16 Oganesian L, Bryan TM. 2007. Physiological relevance of telomeric G-quadruplex formation: a potential drug target. *Bioessays*. 29: 155–165.
17 Izbicka E, *et al*. 1999. Effects of cationic porphyrins as G-quadruplex interactive agents in human tumor cells. *Cancer Res*. 59:639–644.

18 Miller KM, Rodriguez R. 2011. G-quadruplexes: selective DNA targeting for cancer therapeutics? *Expert Rev Clin Pharmacol*. 4: 139–142.

19 Hänsel-Hertsch R, *et al.* 2016. G-quadruplex structures mark human regulatory chromatin. *Nat Genet*. 48:1267–1272.

20 Asamitsu S, Obata S, Yu Z, Bando T, Sugiyama H. 2019. Recent progress of targeted G-quadruplex-preferred ligands toward cancer therapy. *Molecules*. 24:429.

21 Meier-Menches SM, *et al.* 2020. An organometallic gold(I) bis-N-heterocyclic carbene complex with multimodal activity in ovarian cancer cells. *Chem Eur J*. 26:15528–15537.

22 Kench T, *et al.* 2023. Dimeric metal-salphen complexes which target multimeric G-quadruplex DNA. *Bioconjugate Chem*. 34: 911–921.

23 D'Anna L, *et al.* 2023. Salphen metal complexes as potential anticancer agents: interaction profile and selectivity studies toward the three G-quadruplex units in the *KIT* promoter. *Dalton Trans*. 52:2966–2975.

24 Cozzadilo M, Ceschi S, Groaz E, Sturlese M, Sissi C. 2022. G-quadruplexes formation within the promoter of TEAD4 oncogene and their interaction with Vimentin. *Front Chem*. 10: 1008075.

25 Asamitsu S, Bando T, Sugiyama H. 2019. Ligand design to acquire specificity to intended G-quadruplex structures. *Chem Eur J*. 25: 417–430.

26 Zuffo M, *et al.* 2018. More is not always better: finding the right trade-off between affinity and selectivity of a G-quadruplex ligand. *Nucl Acids Res*. 46:e115.

27 Collie WW, Sparapani S, Parkinson GN, Neidle S. 2012. Structural basis of telomeric RNA quadruplex–acridine ligand recognition. *J Am Chem Soc*. 134:2723–2731.

28 Esaki Y, Islam MM, Fujii S, Sato S, Takenaka S. 2014. Design of tetraplex specific ligands: cyclic naphthalene diimide. *Chem Commun*. 50:5967–5969.

29 Maechetti C, *et al.* 2018. Targeting multiple effector pathways in pancreatic ductal adenocarcinoma with a G-quadruplex-binding small molecule. *J Med Chem*. 61:2500–2517.

30 Islam SA, *et al.* 1985. Comparative computer graphics and solution studies of the DNA interaction of substituted anthraquinones based on doxorubicin and mitoxantrone. *J Med Chem*. 28: 857–864.

31 Agbandje M, Jenkins TC, McKenna R, Reszka AP, Neidle S. 1992. Anthracene-9,10-diones as potential anticancer agents. Synthesis, DNA-binding, and biological studies on a series of 2,6-disubstituted derivatives. *J Med Chem*. 35:1418–1429.

32 Singal PK, Iliskovic N. 1998. Doxorubicin-induced cardiomyopathy. *N Engl J Med*. 339:900–905.

33 Zagotto G, *et al.* 2008. Aminoacyl–anthraquinone conjugates as telomerase inhibitors: synthesis, biophysical and biological evaluation. *J Med Chem*. 51:5566–5574.

34 Collie G, *et al.* 2009. Selectivity in small molecule binding to human telomeric RNA and DNA quadruplexes. *Chem Commun*. 48: 7482–7484.

35 Zambre VP, Murumkar PR, Giridhar R, Yadav MR. 2010. Development of highly predictive 3D-QSAR CoMSIA models for anthraquinone and acridone derivatives as telomerase inhibitors targeting G-quadruplex DNA telomere. *J Mol Graph Model*. 29:229–239.

36 Lin Y-H, *et al.* 2016. Selective recognition and stabilization of new ligands targeting the potassium form of the human telomeric G-quadruplex DNA. *Sci Rep*. 6:31019.

37 Molecular Operating Environment (MOE), 2020.09 Chemical Computing Group ULC, 1010 Sherbooke St. West, Suite #910, Montreal, QC, Canada, H3A 2R7 2023.

38 Tseng T-Y, *et al.* 2018. The G-quadruplex fluorescent probe 3,6-bis(1-methyl-2-vinyl-pyridinium) carbazole diiodide as a biosensor for human cancers. *Sci Rep*. 8:16082.

39 Tseng T-Y, Chu IT, Lin S-J, Li J, Chang T-C. 2019. Binding of small molecules to G-quadruplex DNA in cells revealed by fluorescence lifetime imaging microscopy of *o*-BMVC foci. *Molecules*. 24:35.

40 Cohen SM, Lippard SJ. 2001. Cisplatin: from DNA damage to cancer chemotherapy. *Prog Nucl Acid Res Mol Biol*. 67:93–130.

41 Bedrat A, Lacroix L, Mergny JL. 2016. Re-evaluation of G-quadruplex propensity with G4Hunter. *Nucl Acids Res*. 44: 1746–1759.

42 Smogorzewska A, de Lange T. 2004. Regulation of telomerase by telomeric proteins. *Annu Rev Biochem*. 73:177–208.

43 Yuan X, Larsson C, Xu D. 2019. Mechanisms underlying the activation of TERT transcription and telomerase activity in human cancer: old actors and new players. *Oncogene*. 38:6172–6183.

44 Atessahin A, Ceríbaşi AO, Yuce A, Bulmus O, Cikim G. 2007. Role of ellagic acid against cisplatin-induced nephrotoxicity and oxidative stress in rats. *Basic Clin Pharmacol Toxicol*. 100:121–126.

45 Xu H, *et al.* 2017. CX-5461 is a DNA G-quadruplex stabilizer with selective lethality in BRCA1/2 deficient tumours. *Nat Commun*. 8: 14432.

46 Shioda N, *et al.* 2018. Targeting G-quadruplex DNA as cognitive function therapy for ATR-X syndrome. *Nat Med*. 24:802–813.

47 Ashton TM, McKenna WG, Kunz-Schughart LA, Higgins GS. 2018. Oxidative phosphorylation as an emerging target in cancer therapy. *Clin Cancer Res*. 24:2482–2490.

48 Nguyen C, Pandey S. 2019. Exploiting mitochondrial vulnerabilities to trigger apoptosis selectively in cancer cells. *Cancers (Basel)*. 11:916.

49 Falabella M, Fernandez RJ, Johnson FB, Kaufman BA. 2019. Potential roles for G-quadruplexes in mitochondria. *Curr Med Chem*. 26:2918–2932.

50 Huang W-C, *et al.* 2015. Direct evidence of mitochondrial G-quadruplex DNA by using fluorescent anti-cancer agents. *Nucl Acids Res*. 43:10102–10113.

51 Falabella M, *et al.* 2019. G-quadruplex dynamics contribute to regulation of mitochondrial gene expression. *Sci Rep*. 9:5605.

52 Ahmed AA, *et al.* 2020. Asymmetrically substituted quadruplex-binding naphthalene diimide showing potent activity in pancreatic cancer models. *ACS Med Chem Lett*. 11:1634–1644.

53 Jin C, *et al.* 2014. Chem-seq permits identification of genomic targets of drugs against androgen receptor regulation selected by functional phenotypic screens. *Proc Natl Acad Sci U S A*. 111: 9235–9240.